Food Packaging and Shelf Life 34 (2022) 100973

Contents lists available at ScienceDirect

Food Packaging and Shelf Life

journal homepage: www.elsevier.com/locate/fpsl

Finding a carbohydrate gel-based oxygen indicator for expedited detection of defects in metal-oxide coated food packaging

Ashutos Parhi [a,*], Chongyuan Zhang [a], Chandrashekhar R. Sonar [a], Sindhuja Sankaran [a], Barbara Rasco [b], Juming Tang [a], Shyam S. Sablani [a,*]

[a] Department of Biological Systems Engineering, Washington State University, P.O. Box-646120, WA 99164-6120, USA
[b] College of Agriculture and Natural Resources, University of Wyoming, 1000 E. University Ave., Laramie, WY 82071, USA

ARTICLE INFO

Keywords:
Gellan gum
Oxygen indicator
SEM
Food packaging
Shelf life

ABSTRACT

Defects can increase oxygen and water vapor transmission rates (OTRs, WVTRs) of metal-oxide (MO)-coated films, reducing their effectiveness as packaging for shelf-stable foods. These defects are microscopic, can occur at random places in the coating and are highly challenging to locate. This study focused on formulating methylene blue (MB)-containing oxygen indicators based on 1.8% (w/v) agar, Gellan_NaCl, and Gellan_$CaCl_2$. Pouches prepared from two MO-coated multilayer films (A and B) were filled with tap-water, retort-processed for 40 ± 0.2 min (R40) at 121 °C, emptied post-processing, refilled with the oxygen indicators, sealed, and stored at 23 ± 2 °C and 40 ± 0.2 °C for 90 days. Gel-filled pouches were imaged at days 0, 5,10,20,30,60, and 90. Gellan_NaCl showed a higher oxygen sensitivity, lower water release ($P < 0.05$), less MB diffusion than agar and Gellan_$CaCl_2$ and located the defects within 20 days at 40 ± 0.2°C. Overall, the Gellan_NaCl-based oxygen indicator would assist the polymer industry in characterization and development of high-barrier, food-packaging.

1. Introduction

High barrier packaging is a necessity for retaining the shelf life of in-package, sterilized, and shelf-stable foods (Parhi et al., 2020). During in-package thermal processing, the packaging is subjected to 121–125 °C for varying durations (Parhi et al., 2019, 2020). Metal-oxide (MO) coatings in multilayered polymer food packaging can enhance their moisture and oxygen barrier properties. Exposure to high temperatures during thermal processing can create thermal stress-induced defects in the MO-coating layer composed of organic and inorganic materials (Poly acrylic acid, AlO_x, SiO_x), and alter the morphology of the polymer substrate composed of PET, PP or Nylon (Parhi et al., 2019, 2020). The latter can also create defects in the coating layer (Leterrier, 2003; Leterrier et al., 2001). Additionally, mechanical stresses can create cracks and pinholes in the coating as well. Combined together, these factors tend to increase the oxygen and moisture permeability of the packaging and resultingly, lower the packaged products' shelf life.

Commercial MO-coated multilayer films consist of PET layers coated with inorganic oxides like AlO_x, SiO_x, organic compounds such as polyacrylic acid (PAA), or hybrid elements (Parhi et al., 2019, 2020). Conventionally, the MO-coating is present towards the inside of the PET layer, sandwiched further by the nylon 6 and polypropylene (PP) layers, thus forming a multilayered structure (Parhi et al., 2019). While layering improves the barrier and mechanical properties of the packaging, this also makes it harder to locate the defects through traditional microscopic techniques that can only analyze the external film surface (Parhi et al., 2019, 2020).

Secondly, cracks and pinholes can occur at random locations (Parhi et al., 2019, 2020). Coupled with the inability to scan the actual coating surface, this makes detection of the defects difficult. Thirdly, the size of these defects is in the micrometer to nanometer range (Roberts et al., 2002). Common microscopic methods such as SEM, AFM and TEM do not permit scanning larger surface areas required for analysis (sample dimension being in millimeters to centimeters). Therefore, many samples will be required for a proper analysis, making the characterization process complicated and time-consuming (Parhi et al., 2019).

Sensors such as OxyDot® have been used for measuring volumetric oxygen ingress through food packaging (Bhunia et al., 2016). These sensors are small in dimension and cannot detect localized oxygen permeation through multitudes of defects in the MO-coated polymer films (Parhi et al., 2019; Bhunia et al., 2016). Parhi et al. (2019) have developed an oxygen indicator based on 1.5% (w/v) agar gel. The

* Corresponding authors.
E-mail addresses: ashutos.parhi@wsu.edu (A. Parhi), ssablani@wsu.edu (S.S. Sablani).

https://doi.org/10.1016/j.fpsl.2022.100973
Received 29 March 2022; Received in revised form 21 September 2022; Accepted 18 October 2022
Available online 8 November 2022

indicator could successfully locate the defects in MO-coated films at 23 ± 2 ℃ but required 180 days to do so. Additionally, when subjected to elevated temperatures (40 ± 0.2 ℃) with the aim of shortening the detection time, the indicator was unsuccessful in locating the defects. Considering the above-mentioned, a rapid, effective, and easy-to-use indicator is required that can locate the defects and work as a tool to characterize the MO-coated films' barrier performance.

Carbohydrate gelling agents possess a higher gelation temperature, and water-holding capacities and therefore, have been used as carriers and encapsulating agents for food and drug related applications (Tang et al., 1994). To prepare a highly functional oxygen indicator, it was essential to find an inert gel system that can function at elevated temperatures. Hence, Gellan and agar gels were explored in this study.

This study focused on three primary objectives: (i) developing an indicator using food-grade biopolymers with a higher temperature resistance (ii) assessing the oxygen sensitivity of the gels, and (iii) testing the effectiveness of the indicators with actual MO-coated packaging under real-time conditions. Considering these, we experimented with two carbohydrates (three gels): Agar, low-acyl Gellan gum (crosslinking agents-NaCl, and $CaCl_2$). The first step involved formulating the indicators and measuring their pH, water activity (a_w), moisture content, water release (WR), color diffusion, and morphology. The second step involved assessing the oxygen sensitivity of the indicator formulated using the above-mentioned gels. In the third and final step, the indicators were field-tested by using two retort-processed, MO-coated multilayer packaging films at 23 ± 2 ℃ and 40 ± 0.2 ℃ for 90-days.

2. Materials and methods

2.1. Metal oxide (MO)-coated multilayer films

Two MO-coated multilayer polymer films (A and B) were analyzed in this study (Table 4). Both the films had the MO coating towards the inside of the outermost PET layer. Anhydrous dextrose (MW: 180.16 g/mol, MP: 150–152 ℃), sodium hydroxide (NaOH) pellets (MW: 39.9 g/mol), MB (MB) trihydrate powder (MW: 373.9 g/mol), agar powder (pH: 5–8), sodium chloride (NaCl) (anhydrous, free-flowing reagent, purity ≥ 99 %) and $CaCl_2$ powder (anhydrous, free-flowing reagent, purity ≥ 96 %) was procured from Millipore Sigma, St. Louis, MO. Low-acyl Gellan gum powder (*Kelcogel® F*) was provided by CP Kelco. The Gellan gum contained both monovalent and divalent cations, Na^+ (478 mg) and Ca^{2+} (252 mg), respectively (Table 1). Lastly, sucrose fatty acid ester was purchased from TCI (TCI America, Portland, OR).

2.2. Formulation of the indicators

2.2.1. Formulating the indicator using agar

For preparing the oxygen indicator using agar, at first Milli-Q water was boiled in glass beakers for 20–25 min at 98 ℃ (boiling temperature) to reduce the dissolved oxygen in the water. Subsequently, the boiled water was cooled down to 90 ℃ followed by flushing the beaker's headspace with purified nitrogen (99.0 % N_2) to further reduce the presence of oxygen in the headspace. Afterward, the beakers were tightly covered with aluminum foil to minimize oxygen dissolution in the water.

For each 100 mL of water, 1.8 g of agar, 0.1 g of sucrose fatty acid ester, 6 g of dextrose, 0.05 g of sodium hydroxide, and 0.015 g of MB was used. The concentration of agar gel was determined based on prior research where 1.5 % (w/v) agar gel was used to formulate a similar indicator for detecting the defects in the MO-coated films (Parhi et al., 2019). At first, a dry mixture of 2 g of dextrose and 0.1 g of sucrose fatty acid ester was added to 100 mL of deoxygenated water while stirring at a speed of 1100 rpm and at 90 ℃ temperature. Once the mixture was completely dissolved, the remaining 4 g of dextrose was added followed by agar, NaOH, and MB in the above-mentioned amounts. These reagents were added one by one in a sequential manner, once each one of them was properly dissolved in the solution.

2.2.2. Formulating the indicator using Gellan gum

A slightly different approach was followed for formulating the indicators using Gellan gum with NaCl and $CaCl_2$ based crosslinking agents. As was the case with agar, at first Milli-Q water was boiled for 20–25 min in glass beakers at 98 ℃ (boiling temperature). Subsequently, the boiling water was cooled to 23 ± 2 ℃ under 99 % N_2 flush and the beakers were quickly covered with aluminum foil thereafter. Low-acyl Gellan gum powder was slowly added to the water in the beaker and the mixture was stirred at 500 rpm. After five minutes of stirring, the solution attained a semi-solid condition. At that point, the temperature was slowly increased to 96 ℃. The gel started to melt as the temperature increased. The temperature was held constant while stirring the gel solution at 800 rpm until the solution attained a clear form and the active components were added one by one under constant stirring.

For each 100 mL of water, 1.8 g low acyl Gellan gum powder (w/v %) was used. Additionally, for Gellan gel, 2.05 g of NaCl (350 mM) and 0.09 g (8 mM) of $CaCl_2$ were used. The amount of Gellan gum, and the crosslinking agents was determined based on prior research where 1.8% (w/v) Gellan gum had shown better mechanical properties (Tang et al., 1994). For formulating Gellan gel-based indicators, the other reagents were added in the same manner and in the same amount and sequence, as it was the case of agar once the Gellan gum melted completely in the hot water (the gel ran clear without any lumps) and the water temperature was lowered to 90 ℃. The cross-linking reagents (NaCl or $CaCl_2$) were added to the solution once MB got dissolved in the solution. Stirring was maintained at the same speed and temperature for five more min after the salts were added. Subsequently, the hot gel solution was

Table 1
Physicochemical properties of the biopolymers used for formulating the oxygen indicator.

Gels (1.8% w/v)	Crosslinking agent	Percentage of additives in gel matrix (per 100 g of dry gel powder)								pH		Water activity (a_w)	Moisture content (%)
		Ca* (mg)	P* (mg)	Fe* (mg)	Mg* (mg)	Na* (mg)	K* (mg)	Ash* (g)	Moisture* (g)	23 ± 2 °C	40 ± 0.2 °C	25 ± 0.1 °C	55 °C
Agar	NR	NA								6.08 ± 0.04^A	5.77 ± 0.04^A	0.936 ± 0.002^A	91.7 ± 1.01^A
Low acyl Gellan gum	NaCl	252	115	4	91	478	4650	10	7	6.34 ± 0.23^A	5.55 ± 0.01^B	0.933 ± 0.004^A	89.3 ± 0.09^B
	$CaCl_2$									6.38 ± 0.07^A	5.47 ± 0.01^C	0.937 ± 0.002^A	91.3 ± 0.2^A

Note: * shows the information is obtained from the manufacturers; NA: Not available; NR: Not required. Values are in mean ± standard deviation. Significant differences ($P < 0.05$) between values within columns are presented by uppercase superscripts.

poured into the polymer pouches.

2.3. Packaging and storage

The liquid gel solutions were poured into the processed and unprocessed pouches, sealed immediately (within 10 s) with an impulse sealer (sealing time 6.5 s) with as minimum headspace as possible, and stored at 23 ± 2 ℃ and 40 ± 0.2 ℃ and 20 ± 4% RH for 90 days. For each type of packaging and each type of gel, we prepared samples in triplicate. The packaged gel samples were imaged at days 0, 5, 10, 20, 30, 60, and 90.

2.4. Image acquisition

Images were acquired using a phenotyping box constructed from a cardboard box and equipped with a digital camera (12.1 megapixels, PowerShot SX260, Canon U.S.A. Inc., Huntington, NY). The inner wall of the box was covered with white paper to ensure uniformity in light reflection. A pair of fluorescent white lights were mounted on the inner wall of the top panel of the box. Samples were placed at a fixed location and the distance between samples and camera lens was kept constant. A reflectance reference panel (99.9 % reflectance, Spectralon Diffuse Reflectance Standard, SRT-99–020, Labsphere, North Sutton, NH) was placed next to the samples during image acquisition and used for radiometric calibration.

2.5. Physicochemical properties

2.5.1. pH

The pH of the three gels was measured as described in (Parhi et al. (2019) in triplicate at 23 ± 2 ℃ and 40 ± 0.2 ℃ using a SevenGo™ SG2 pH meter (Mettler-Toledo AG, 8603 Schwerzenbach, Switzerland). At first, the pH meter was checked for accuracy using three standard stock solutions with pH values of 4.0, 7.0 and 10.0. Subsequently, the actual samples were tested. Thirty mL of the hot gel was poured into fifty mL polypropylene centrifuge tubes and allowed to form the gel at 23 ± 2 °C. Once the gels were formed, they were stored at 23 ± 2 °C and 40 ± 0.2 °C for further 24 h prior to pH measurements in order for the gels to reach the temperatures.

2.5.2. Water activity (a_w) and moisture content

The a_w was measured in triplicate at 25 ℃ as per Parhi et al. (2019). The moisture content was evaluated by drying triplicate of 5 g of solidified gel sample in aluminum foil pans for 72 h at 55 ℃ in a hot air oven. The drying time was estimated based on prior research with agar and Gellan gels (Cassanelli et al., 2019; Parhi et al., 2019). In addition, the time of drying was validated by measuring the weight of the samples at regular intervals to ascertain no change in the weights after 72 h of drying time.

2.6. Oxygen sensitivity

The oxygen sensitivity was quantified in duplicate by measuring the color change in the gels when exposed to atmospheric oxygen. Freshly prepared hot gels (approx. 50–80 mL) were poured into 100 mm diameter Petri dishes. The gels changed color with oxygen exposure. The gel-containing petri-dishes were imaged after 0, 5, 10, 15, 20, 30, 45, and 60 min of pouring the hot gel. We acquired the images of the petri dishes containing the three gels as detailed in Section 2.4. Once the images were acquired, they were processed in custom image processing algorithm developed MATLAB (The MathWorks, Natick, MA). Images acquired were first radiometrically calibrated with the reference panel. Region of interest (ROI) for each petri dish was generated. The color space of ROI was converted from RGB (red-green-blue) to CIE $L^*a^*b^*$, in which the color features (L^*: lightness, a^*: red-green color component, b^*: blue-yellow color component) were extracted. The total color change (ΔE) was calculated using Eq. 1.

$$\Delta E = \sqrt{(\Delta L^*)^2 + (\Delta a^*)^2 + (\Delta b^*)^2} \quad (1)$$

2.7. Water release (WR)

WR in the gels was measured in duplicate by filling thirty mL of liquid gel into fifty mL plastic centrifuge tubes. The tubes were closed by applying vacuum grease and further wrapped with plastic adhesive tapes to minimize moisture loss. Afterward, they were kept at 23 ± 2 ℃ for 24 h for complete gelation. Subsequently, the tubes were stored at 23 ± 2 ℃ and 40 ± 0.2 ℃ for 90-days. The WR in the gel samples were measured at days 10, 30, 60, and 90 with wiping and centrifugation followed by wiping per (Banerjee & Bhattacharya, 2011; Mao et al., 2001). Water from the top of the gels was gently wiped and the tubes were weighed immediately thereafter. For centrifugation, the tubes were centrifuged at 5000 rpm (2670 *g*) for 10 min in an AccuSpin 400 centrifuge (Fisher Scientific, PA, USA) and weighed immediately after wiping off the released water. The initial weights of the tubes were measured at 23 ± 2 ℃ once the polymers were gelled andthe WR was calculated (Banerjee & Bhattacharya, 2011).

2.8. Diffusion of oxidized methylene blue (MB)

The diffusion of oxidized MB was assessed by preparing a duplicate of packaged gel samples containing two layers of the gel: the top layer with MB, and the bottom layer without. 175 mL of each gel (without MB) was poured at first into the retort processed film B pouches and kept at 23 ± 2 ℃ for 24 hr for complete gelation. Afterward, another 175 mL of the hot gel (with the MB) was poured on top of the layer with no MB. The second gel layer was also kept at 23 ± 2 ℃ for 24 h. Subsequently, the pouches were stored at 40 ± 0.2 ℃ to study the MB diffusion. The pouches were loosely sealed with adhesive tapes during storage to allow constant oxygen exposure and minimize moisture loss. Samples were imaged once every 7-days for 28 days to assess the MB diffusion.

2.9. Scanning electron microscope (SEM)

For SEM analysis, gel samples (1 × 0.5 × 0.5 cm^3) were extracted and immediately dipped into liquid nitrogen and subsequently freeze-dried for 30 h at − 55 ℃. The dried gel samples were gold-coated using a sputter coater (Hummer 6.6 sputter system, CA). Triplicate of the coated gel samples ($N > 10$) were analyzed with an SEM (FEI Quanta 200 F, Thermo Scientific Quanta, Hillsboro, OR) under a high vacuum (accelerating voltage: 20 KV, spot size: 3.0, detector: ETD).

2.10. Thermal processing

Pouches prepared from the MO-coated films were filled with 250 mL of food simulant (tap water), vacuum packed (vacuum level: 99%; sealing time: 3–5 s) and processed for 40 ± 0.2 min at 121 ℃ in a pilot-scale retort system (R40) (Allpax Products, Seymour Meyers Blvd., LA) (come-up time: 10 min, pressure cool: 5 min, atmospheric cool: 2 min, operation mode: spray-water). The thermal processing time was determined based on the solid food products such as fish packed into flexible pouches to attain an F_0 of 6–9 min at the geometric center of the pouch (Mohan et al., 2006; Parhi et al., 2019).

2.11. Oxygen and water vapor transmission rates (OTRs, WVTRs)

The OTR and WVTR values were adopted from (Parhi et al., 2019). The films' OTRs and WVTRs were measured in triplicate as per Parhi et al. (2019). Film samples measuring 50 cm^2 in area were extracted from pouches before and after retort processing and mounted onto the MOCON Ox-Tran 2/21 MH and Permatran 3/33 MG (Modern Control, Minneapolis, MN). The OTRs of the films were measured at 23 °C, 1 atm

pressure and 55 ± 1% RH while WVTRs were measured at 100% RH and 38 °C. The OTRs and WVTRs were measured in cc/m^2.day and g/m^2. day, respectively.

2.12. Statistical analysis

The results were compared along rows and columns for significant differences ($P < 0.05$) at $\alpha = 0.05$ using a CRD model with Tukey's HSD in SAS university edition.

3. Results and discussion

3.1. Gel properties

3.1.1. pH

The agar gel-based indicator had a pH of 6.08 at 23 ± 2 ℃, while indicators with Gellan_NaCl and Gellan_$CaCl_2$ gels had pH of 6.34 and 6.38, respectively (Table 1). At 40 ± 0.2 °C, agar, Gellan_NaCl, and Gellan_$CaCl_2$ had pH of 5.77, 5.55, and 5.47, respectively (Table 1) ($P < 0.05$). All the gels had a higher pH at 23 ± 2 °C than 40 ± 0.2 °C. This could be due to higher oxygen diffusion through the gels at 40 ± 0.2 °C, inducing a faster reaction (Bhunia, Sablani, et al., 2016). Glucose is one of the active elements in the redox reaction causing the color change (Anderson et al., 2012; Campbell, 1963; Parhi et al., 2019). At the end of the reaction, arabinonic acid is generated in the gels, which could be responsible for the occurrence of pH drop (Anderson et al., 2012; Campbell, 1963). At 40 ± 0.2 ℃, higher oxidation and a faster reaction rate may have generated more arabinonic acid in the gels, causing the pH drop (Anderson et al., 2012; Campbell, 1963).

The pH can influence the gels' microstructure as well as the number of the junction zones present in the gels, thus affecting the gel strength and in turn, the detection ability of the indicators (Picone & Cunha, 2011). In case of Gellan gum, a lower pH can result in more homogeneity in the gels (Picone & Cunha, 2011). In previous studies, gellan gels with a pH of 7 had shown a flat and closed network. The porosity in Gellan gels decreased at the pH of 5.3 and 3.5, with the latter having a highly continuous interface containing smaller pores (Picone & Cunha, 2011). Secondly, Gellan gels tend to have a lower gel strength at higher pH due to the formation of fewer junction zones (Picone & Cunha, 2011). In this study, at 23 ± 2 °C, there was no significant difference ($P > 0.05$) between the pH of the three gels. At the same time at 40 ± 0.2 °C, both the Gellan_NaCl and Gellan_$CaCl_2$ had significantly lower pH than agar ($P < 0.05$) and Gellan_NaCl had a higher pH than Gellan_$CaCl_2$. This was contrary to the morphological properties where Gellan_NaCl showed a less porous structure. This could be due to the molecular network present in the respective gels that involvs monovalent and divalent cations. As a result, despite a higher pH, Gellan_NaCl showed a less porous structure than the Gellan_$CaCl_2$. Consecutively, the gel had a reduced diffusion of oxidized MB than Gellan_$CaCl_2$, as explained in the subsequent sections.

3.1.2. Water activity (a_w) and moisture content

Both agar and gellan gum are hydrocolloids, hence their molecular network holds water by entrapping the water molecules within the chain systems. In this study, we are exposing these gel systems to 23 ± 2 ℃ and 40 ℃ for 90 days to assess the water release and color change, both of which are directly dependent on the amount of water released due to the breaking down of the molecular network as well as the amount of water contained in these gel systems. The water activity and moisture content measurements provided more understanding about the unbound and the total water contained in the gel systems, respectively. In addition, this study focused on assessing the crosslinking potential of NaCl and $CaCl_2$. Thus, measuring the a_w and moisture content of the gels provided a wholesome picture of the efficiency and functionality of the indicator system at 23 ± 2 ℃ and 40 ℃.

Water activity for agar was 0.936, while Gellan_NaCl and Gellan_$CaCl_2$ had a_w 0.933 and 0.937, respectively (Table 1). Agar had the highest moisture content of 91.7% following Gellan_$CaCl_2$ (91.3%) and, Gellan_NaCl (89.3 %) (Table 1) ($P < 0.05$). Hydrocolloids such as the ones used in this study act as matrices that hold the entrapped water and active elements within their molecular network (Bhunia, Sablani, et al., 2016). This water can be released when the gel network weakens upon exposure to elevated temperatures (40 ℃). Hence, it is possible for the indicators to get influenced by the moisture content of the gels. In this study, Gellan_NaCl gel showed a significantly lower ($P < 0.05$) moisture content than the other gels (Table 1). This may have resulted in a lower WR.

3.2. Oxygen sensitivity

The oxygen sensitivity was assessed based on the rate at which the gels changed color (ΔE and b^*) with oxygen exposure (Fig. 1). Gellan_NaCl showed the highest change in color with time. The total color change (ΔE) for Gellan_NaCl increased by 10.9 (from 33.0 to 43.9). For agar, the ΔE increased from 28.8 to 37.7 (a change of 8.9) while in the case of Gellan_$CaCl_2$, the values increased from 9.71 to 18.64, a change of 8.93 after exposure to the atmospheric oxygen for 60 min. Color change in Gellan_NaCl was higher at each time point followed by agar and Gellan_$CaCl_2$, although both agar and Gellan_$CaCl_2$ showed a similar change in total color change (ΔE) with increasing time. This demonstrates that the Gellan_NaCl changed color faster than the other two gels. Thus, it was more sensitive towards oxygen exposure.

In case of b^*, which represents the chromaticity index yellow to blue (+ve to -ve), Gellan_NaCl showed increasingly blue color than both agar and Gellan_$CaCl_2$. Initially, at the time point of 0 min, the Gellan_$CaCl_2$ was bluer than Gellan_NaCl and agar. However, 5 min of exposure to atmospheric oxygen resulted in a rapid increase in the blueness of the NaCl gel followed by Gellan_$CaCl_2$ and agar. This trend was consistent throughout all the data points and continued until the end of measurements (60 min). Agar had the least blue color among the three gels. This illustrated that Gellan_NaCl performed better than agar and Gellan_$CaCl_2$.

Ideally, the gels themselves should have very limited to no interference on the sensitivity and redox reaction in the indicator. Additionally, the hydrocolloid system must also provide the necessary stability required for enhanced functionality of the indicator and, if possible, aid in accelerating the detection process of the defects. Prior research has shown that low acyl Gellan gel with divalent crosslinking agents such as $CaCl_2$ and $MgCl_2$ tend to have a higher gelation point and higher thermal and mechanical stability compared to Gellan gel with monovalent crosslinking agents such as NaCl and KCl (Mao et al., 1999; Tang et al., 1994, 1995, 1997). In this case, the entire surface of the gel-containing petri dishes was exposed to the atmospheric oxygen. Gellan_$CaCl_2$ was less oxygen sensitive than agar and Gellan_NaCl. This could be due to the difference in the gel microstructures. This is explained in the subsequent sections as well.

The tests for oxygen sensitivity were performed at 23 ± 2 ℃ and with complete exposure to the atmospheric oxygen. Subsequently, two MO-coated pouches were filled with the gels and stored at 23 ± 2 ℃ and 40 ± 0.2 ℃ to study their applicability under actual conditions. Color change in the pouched gel samples varied based on the storage temperature, oxygen, and water vapor permeabilities of respective pouches, water release, and color diffusion.

3.3. Water release (WR)

The WR from the gels was measured after storage at 23 ± 2 ℃ and 40 ± 0.2 ℃ for 90 days (Tables 2–3). Gellan_NaCl showed a lower WR than agar and Gellan_$CaCl_2$ at both the temperatures. Agar had a higher WR among the three gels for all the temperatures as measured by both the methods. This could be due to the higher gelation temperature of Gellan gum crosslinked by the mono and divalent cations compared to

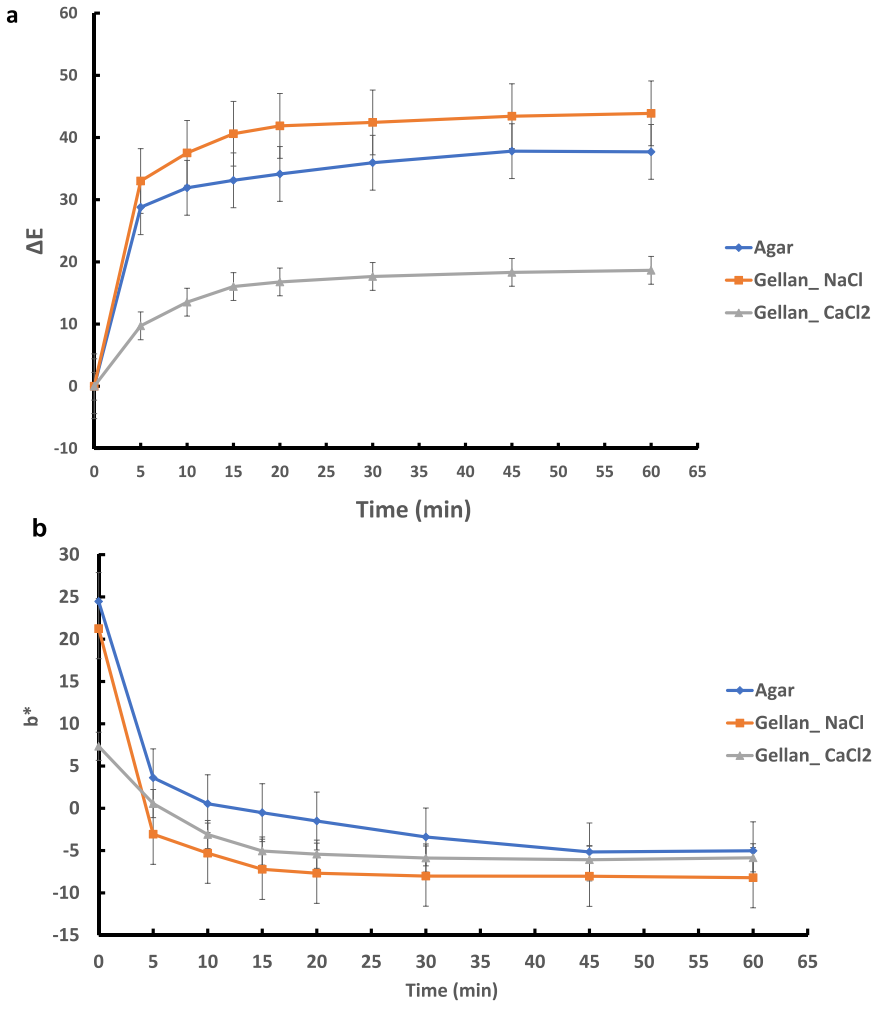

Fig. 1. Oxygen sensitivity of the gels; a and b represent the variation in total color change (ΔE) and b^*, respectively.

Table 2
Water release (WR) from the gels at 23 ± 2 °C measured by wiping.

Gels	Water release (%)							
	23 ± 2 °C				40 ± 0.2 °C			
	Day 10	Day 30	Day 60	Day 90	Day 10	Day 30	Day 60	Day 90
Agar	1.69 ± 0.18^{aA}	1.35 ± 0.06^{aA}	1.42 ± 0.15^{aA}	1.58 ± 0.09^{aA}	1.73 ± 0.10^{aA}	1.75 ± 0.10^{aA}	1.71 ± 0.05^{aA}	1.52 ± 0.02^{bA}
Gellan_NaCl	0.35 ± 0.08^{abB}	0.57 ± 0.12^{aB}	0.19 ± 0.01^{bcB}	0.15 ± 0.05^{cB}	0.61 ± 0.02^{aB}	0.39 ± 0.06^{bB}	0.57 ± 0.01^{aC}	0.58 ± 0.05^{aC}
Gellan_$CaCl_2$	0.46 ± 0.14^{aB}	0.11 ± 0.06^{bC}	0.07 ± 0.03^{bC}	0.07 ± 0.00^{bB}	0.66 ± 0.14^{aB}	0.92 ± 0.30^{aB}	0.90 ± 0.14^{aB}	0.81 ± 0.01^{aB}

Note: Values are in Mean ± standard deviation; Significant differences ($P < 0.05$) between values within rows and columns are presented by lowercase and uppercase superscripts, respectively.

Table 3
Water release (WR) from the gels at 23 ± 2 °C measured by centrifugation.

Gels	Water release (%)							
	23 ± 2 °C				40 ± 0.2 °C			
	Day 10	Day 30	Day 60	Day 90	Day 10	Day 30	Day 60	Day 90
Agar	2.52 ± 0.31^{aB}	1.28 ± 0.20^{bA}	1.69 ± 0.85^{abA}	2.12 ± 0.26^{aA}	1.78 ± 0.14^{aC}	1.28 ± 0.18^{aA}	1.16 ± 0.27^{aA}	1.28 ± 0.28^{aA}
Gellan_ NaCl	0.55 ± 0.78^{bA}	2.04 ± 0.82^{abA}	3.01 ± 0.06^{aA}	0.35 ± 0.34^{bB}	3.40 ± 0.03^{aB}	0.50 ± 0.26^{bB}	0.63 ± 0.18^{bA}	0.69 ± 0.11^{bA}
Gellan_ $CaCl_2$	3.30 ± 0.03^{aC}	1.85 ± 1.47^{aA}	3.27 ± 0.30^{aA}	2.04 ± 1.56^{aAB}	3.27 ± 0.03^{aA}	0.87 ± 0.15^{bAB}	0.94 ± 0.03^{bA}	1.32 ± 0.32^{bA}

Note: Values are in Mean ± SD; Significant differences ($P < 0.05$) between values within rows and columns are presented by lowercase and uppercase superscripts, respectively.

agar. In Gellan gels, presence of crosslinked networks imparts additional strength to the gel. In this study, it was also observed that agar gel had a lower hardness compared to the Gellan gels. Although, the strength and water holding capacities varied between the Gellan gums containing mono and divalent cations, they were invariably stronger than agar and tended to have a lower WR as well.

Water from the gels is released when the bonds in a completely formed gel network are weakened (Mao et al., 2001; Nishinari & Fang, 2016). This typically happens when a gel is exposed to temperatures exceeding its gelation point, which depends on the gel concentration and type of the gelling agent used. In a completely formed gel, the hydrocolloid network of bonds holds the entrapped water molecules in the gel matrix. When these junction zones forming the 3-dimensional network of bonds weaken at temperatures exceeding the gelation temperature, the entrapped water molecules can leach out (Banerjee & Bhattacharya, 2011; Mao et al., 2001). This is influenced by the presence of sugars such as sucrose and glucose, the type of gelling agent, and the type of crosslinking agent used (Banerjee & Bhattacharya, 2011; Mao et al., 2001). The latter is particularly true for Gellan gums. Prior research has shown that Gellan gum with Ca^{2+} is stronger than Gellan gum formed with monovalent crosslinking cations such as Na^{+}. This was due to their larger size which can influence the electromagnetic strength of the cations (Tang et al., 1995).

In this study, the gels act as a host for the active elements, facilitating the redox reaction to occur while remaining inert themselves. Upon oxygen ingress through the defects in the MO- coating, MB undergoes oxidation and regains its blue color. As more and more oxygen permeate through the defects, a higher blue color results. At that time, the gels' inherent WR comes into the picture. With the gels having higher WR, the water leached tends to act as a carrier and spreads the oxidized MB across the whole gel-containing package. The process occurs faster at 40 ± 0.2 ℃ than 23 ± 2 ℃ due to three reasons: increased oxygen ingress through the packaging films, higher oxygen diffusion throughout the gel, and higher WR. While the oxygen ingress is dependent on the film properties, oxygen diffusion through the gel can increase with the temperature due to the higher diffusivity at elevated temperatures (Bhunia et al., 2016). This is aided by the increased dissolution of oxygen in water, which also affects the diffusion of MB. Water leached from the gels can carry oxidized MB throughout the gel matrix, causing blue coloration. This can significantly hinder the detectability of the indicator since locations with no barrier deterioration can also change color due to the leached-out MB.

3.4. Diffusion of oxidized MB

The MB present in the gels remains in a reduced state until it reacts with the atmospheric oxygen permeated through the defects in the MO coatings and attains its blue form. Fig. 2(a) shows the diffusion of the MB through the three gels at the beginning and end of 28 days of storage at 40 ± 0.2 ℃.

On day 0, both Gellan_NaCl and agar showed a higher blue color in the top layer that contained MB. This could be due to a higher oxygen diffusion through the gels. Gellan_$CaCl_2$ had comparably lower blue coloration in the top layer on day 0. By day 28, all the gels changed color completely in the top layer. The bottom layer, however, was different for three gels. Gellan_$CaCl_2$ showed higher color change in the bottom layer containing the gel without MB. At the same time, the pouches with Gellan_NaCl and agar gels performed better and had lower color diffusion. Especially, the color diffusion in Gellan_NaCl was lower than agar, as evident with the greater amount of gel in the bottom portion with yellow color (Fig. 2(a)). For this experiment, film B which had a higher oxygen barrier compared to film A was used. Hence, whatever oxygen ingress happened, it must have occurred through the top of the pouches which had been loosely sealed with paper tape to ensure adequate access to oxygen during the storage. The color diffusion results will be further corroborated by the color change in the packaged gels, as discussed in the subsequent sections of this paper.

The test illustrated the effects of MB on the performance of the indicator and its ability to effectively detect the cracks. Prior research has also observed similar results with 1.5 % w/v agar where the authors observed increased blueness in the indicator packaged with low barrier films (Parhi et al., 2019). Since the agar concentration was even lower than the present study, a higher blue coloration was observed in the indicator after storage at 40 ± 0.2 ℃. The overall effectiveness of the indicator reduced due to increased number of false-positive locations, where the packaging film changed color despite there being no defects in the MO coating layer.

In the present study, increased concentration of the gelling agents in the indicator effectively reduced the diffusion of the oxidized MB. At the same time, the use of Gellan_NaCl as the gelling matrix lowered the MB diffusion as well. This can be directly correlated with the WR from the gels. Gellan_NaCl showed relatively lower water release compared to both agar and Gellan_$CaCl_2$. With less release of the moisture, the overall water available to act as a carrier for the oxidized MB would also be less. Consequently, the spread of the MB after oxidation would be limited, resulting an effective indicator that can operate at elevated temperatures enabling rapid detection of the defects.

3.5. Gel microstructure

SEM micrographs showed Agar gel to be consisting of larger pores than both Gellan_NaCl and Gellan_$CaCl_2$ (Fig. 2(b)). This could be due to the lack of any crosslinked network in agar unlike the Gellan gels. At the same time, Gellan_NaCl had fewer pores than Gellan_$CaCl_2$. Gellan gels can be composed two microstructures. The first contributes towards the water release from the gel network and is independent of the $CaCl_2$ concentration. The second microstructure is responsible for providing mechanical strength to the gel and is dependent on $CaCl_2$ concentration (Mao et al., 2001). Larger pores were observed with thick network strings while smaller pores could be formed by the thinner web

Table 4
MO-coated films' structure and oxygen and moisture barrier properties.[1]

Films	Thickness (μm, N = 5)	Composition of the layers[2]	Pouch dimension (cm × cm)	Oxygen transmission rate (cc/m^2.day) at 23 °C and 55 ± 1% RH		Water vapor transmission rate (g/m^2.day) at 38 °C and 100% RH	
				Control	R40	Control	R40
A	92.6 ± 0.9	Metal-oxide-coated-PET (12 μm)[3]// ONy (15 μm)//CPP (50 μm)	18.5 × 13	0.04 ± 0.02^{bAB}	0.86 ± 0.18^{aA}	0.11 ± 0.01^{bC}	0.32 ± 0.08^{aB}
B	92 ± 0.7	Overlayer/SiO_x-coated PET (12 μm)// ONy (15 μm)//CPP (60 μm)	18 × 13	0.01 ± 0.01^{bB}	0.09 ± 0.02^{aB}	0.11 ± 0.01^{bC}	0.61 ± 0.11^{aB}

Note: Values are in Mean ± standard deviation; Significant differences ($P<0.05$)between values within rows and columns are presented by lowercase and uppercase superscripts, respectively. The pouches were stand-up and each of them contained 350 mL of liquid gel.

[*] The data was adopted from Parhi et al., (2019)

[a] ONy: Biaxially oriented Nylon 6; CPP: cas tpolypropylene; SiOx: Silicon oxide

[1] Type of MO-coating is not available for this film.

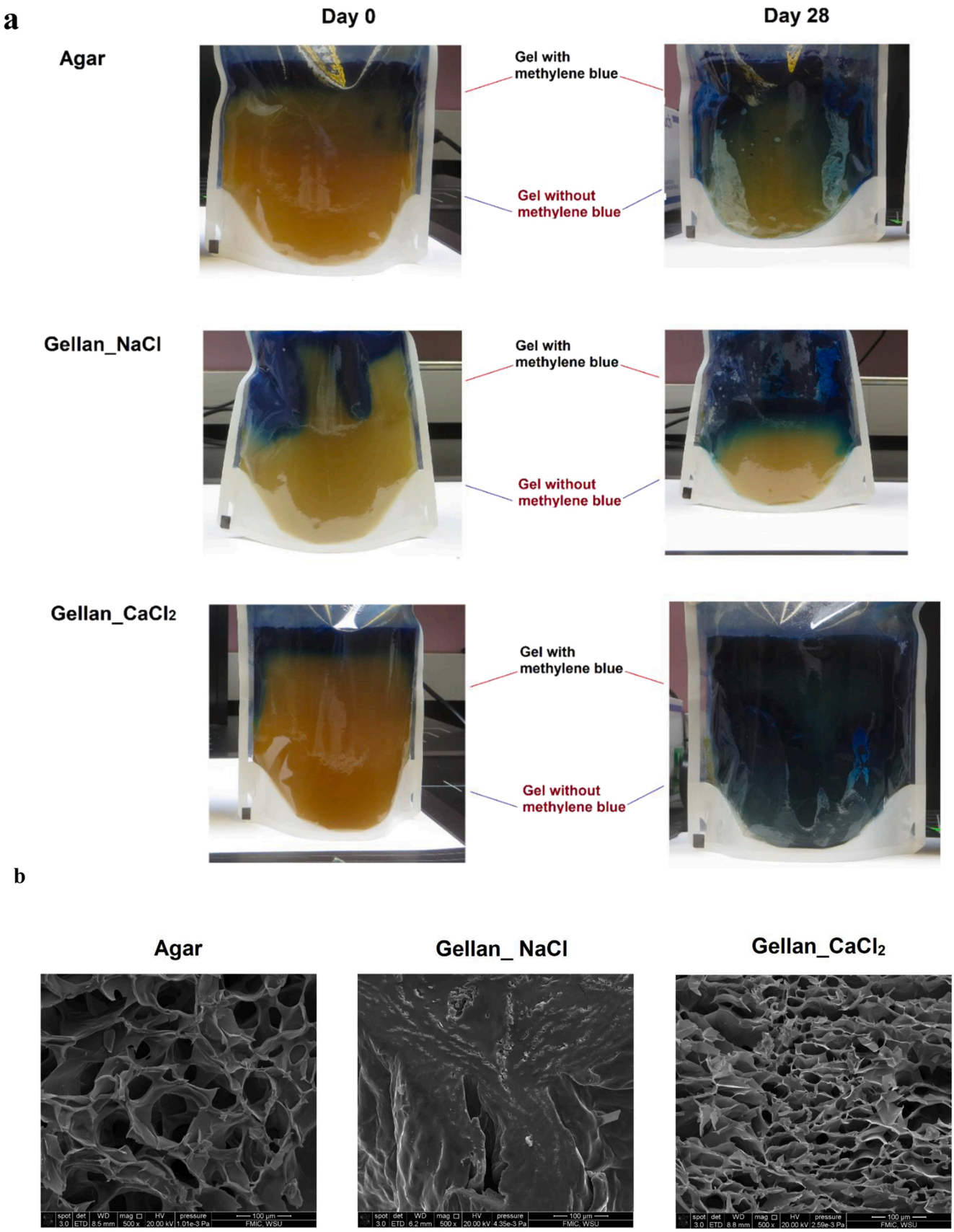

Fig. 2. Diffusion of oxidized methylene blue through the three gels after storage at 40 ± 0.2 ℃ for 28 days and scanning electron microscope (SEM) images of the gel samples at a maginification of 500 X as depicted by a and b, respectively.

structures (Mao et al., 2001). The smaller cations in NaCl could have contributed more towards the thinner webs, resulting in a less porous structure. This would have culminated in a higher surface availability of the MB, resulting in Gellan_NaCl to have a faster color change. At the same time, the larger Ca^{2+} ions in Gellan_$CaCl_2$ with higher ionic strength may have caused larger pores in the gel due to a stronger crosslinked network, resulting in a lower availability of the MB at the surface.

3.6. OTRs and WVTRs of the MO-coated films

Prior to the retort processing, films A and B had very low OTRs: 0.04 and 0.01 cc/ m^2.day, respectively. After 40 min of retort processing (R40), the films' OTRs increased significantly ($P < 0.05$). In case of Film A, the OTR increased from 0.04 to 0.86 (approximately by 22 times) and film B the increase was by 9 times (from 0.01 to 0.09 cc/m^2.day). The presence of an overlayer in film B may have protected the MO-coating from defects such as pinholes and cracks.

In MO-coated multilayer films, both the coating as well as the polymers contribute towards changes in the oxygen and moisture barrier after thermal processing. The MO coating acts as a physical barrier against oxygen permeation (Henry et al., 2001; Parhi et al., 2020). When the MO layer has any defects (macro, nano or lattice defects), oxygen permeation increases (Parhi et al., 2020; Roberts et al., 2002). Researchers have observed that the oxygen permeation primarily occurs through the macro defects (> 1 nm) in the metal oxide (MO) coating (Roberts et al., 2002). The MO-layer can develop these defects from thermal and mechanical stress exposure during retort and MATS processing under high moisture and temperature environment, leading to an increase in the oxygen permeability through the films (Parhi et al., 2020).

High heat and moisture exposure for prolonged periods during thermal processing can alter the morphological properties such as free volume and crystalline fractions of the polymer substrates in the MO-coated films (Parhi et al., 2019). Resultingly, OTR increases following thermal processing. Additionally, these changes in the polymers can also affect the MO-coating. The polymer layers tended to become increasingly brittle after processing, due to moisture absorption during retort process and subsequent release (Bhunia et al., 2016; Parhi et al., 2020). Nylon 6, which enhances the mechanical strength and puncture resistance of the multilayer films, is particularly susceptible to moisture absorption. Nylon 6 layer in the unprocessed films is generally present in a biaxially oriented state. Moisture absorption during processing induces plasticization and release of the absorbed moisture after processing can cause Nylon 6 to lose its oriented state. This makes the films brittle and increases the possibility of occurrence of cracks and pinholes in the deposited MO-layer. Furthermore, thermal processing can initiate thermal expansion (up to the T_g), followed by shrinkage and loss of orientation in the polymers (until melting point) and again shrinkage upon cooling (Leterrier et al., 2001; Parhi et al., 2020). In terms of changes in the coating layer itself, shrinkage during thermal processing (heating and subsequent cooling) can create defects along with other factors, such as the presence of anti-blocking particles on PET surface, coating thickness, and surface roughness of the substrate (Parhi et al., 2019).

The films' WVTRs showed a significant increase ($P < 0.05$) after retort processing. Both the films had the same WVTRs in the unprocessed condition. Interestingly, WVTR of film A had a lower change (2.9 times) than film B (5.5 times) after R40. In MO-coated films, the permeation of moisture is dependent on the interaction between the water molecules and the deposited coating, presence of defects in the coating, and the presence and effectivity of hydrophobic polymers in the multilayered film structure (Henry et al., 2001; Parhi et al., 2019). Although the occurrence of defects may not be of a higher significance in changing the WVTRs of the films, it may still be contributing towards the overall increase in WVTR after thermal processing.

3.7. Color change in the gel-filled pouches

The gels in the pouches changed color from yellow to blue with oxygen ingress during storage, indicating the locations of the defects (Fig. 3). The intensity of the color change varied across the films with storage conditions, their respective OTRs and WVTRs, types of the packaged gel, and the efficiency of the MO-coating in terms of developing defects such as cracks and pinholes. Also, the gel-filled pouches changed color with time, as the defects allowed increasingly higher oxygen to permeate through, especially at 40 ± 0.2 ℃, since elevated temperatures accelerated the oxygen permeation (Bhunia et al., 2016). At the same time, storage at 40 ± 0.2 ℃ facilitated the earlier detection of smaller pinholes and other defects.

The intensity of blueness also varied based on the gel properties and OTRs and WVTRs of the films. Film A with higher OTRs after 40 min of retort processing showed blue color of higher intensity than film B. Secondly, agar and Gellan_$CaCl_2$ turned higher blue color than Gellan_NaCl at 40 ± 0.2 ℃ after 90 days. By the end of 90 days at 23 ± 2 ℃, the color change between the gels was specific to the location of defects, unlike throughout the gels as observed at 40 ± 0.2 ℃. Interestingly, color change in Gellan_NaCl occurred more quickly with the defects detectable by day 5. Even the smaller pinholes were visible by day 5, like the oxygen sensitivity measurements. This was followed by agar and lastly, Gellan_$CaCl_2$ gel. The latter was successful in detecting the larger defects but failed with smaller pinholes.

The color change at 40 ± 0.2 ℃ was more pronounced than at 23 ± 2 ℃ during 90-days of storage. This was indicative of increased oxygen diffusion at higher temperatures. At 40 ± 0.2 ℃, almost of the defects were located by day 20 in pouch A, including the smaller pinholes with Gellan_NaCl. At 23 ± 2 ℃, similar results were observed after day 60 days of storage. Agar and Gellan_$CaCl_2$ were even slower than that at 23 ± 2 ± 2 ℃. This indicated that the accelerated method successfully reduced the detection time by a third of that needed at 23 ± 2 ℃. An intense color change in agar gel by day 10 of the storage at 40 ± 0.2 ℃ was observed. This prevented successful visible detection of defects in those pouches. For Gellan_$CaCl_2$ this happened by day 60. In both these gels, high intensity of the blue coloration prevented locating the smaller pinholes effectively.

For an indicator to be effective, it needs to change its color at the exact locations of the defects but not throughout the gel matrix (Parhi et al., 2019). In case this does not happen, it can cause false-positive identification of the defects due to color change in the gel at locations without any defects. It is significant in films such as film A, where a high OTR can cause higher color change. A gel matrix with higher WR, oxygen diffusivity, and color diffusion can lead to coloration at the locations without any defects (Parhi et al., 2019). A higher WR would create an increased color diffusion through the gel as the released water would act as a carrier to spread the oxidized MB throughout the gel matrix (Parhi et al., 2019). A higher oxygen diffusivity in the gel matrix would result in the gel changing color throughout in a rapid manner. This would prevent successful identification of defects as the chemical reaction will happen throughout the gel, even before all the defects are identified. This is especially significant for the small defects such as pinholes where it takes some time before changing color. Hence, this would affect the accuracy of the method, especially in the low oxygen barrier films. Previously, researchers have analyzed the oxygen diffusivity through the gel matrices and observed that 2% (w/v) agar gel had higher oxygen diffusivity than Gellan gel (crosslinking agent: Mg^{2+}). Also, prior research have suggested that Ca^{2+} can be a better crosslinking agent than Mg^{2+} (Tang et al., 1994, 1997). Hence, from all perspectives, Gellan gels are better suited as the gelling matrix for the oxygen indicator.

Secondly, the packaging films' OTRs and WVTRs had an impact on the color change. As explained previously, the OTRs of film A increased by 22 times after R40 and that of film B by 9 times. Consequently, film A had higher oxygen permeation through the barrier layer than film B.

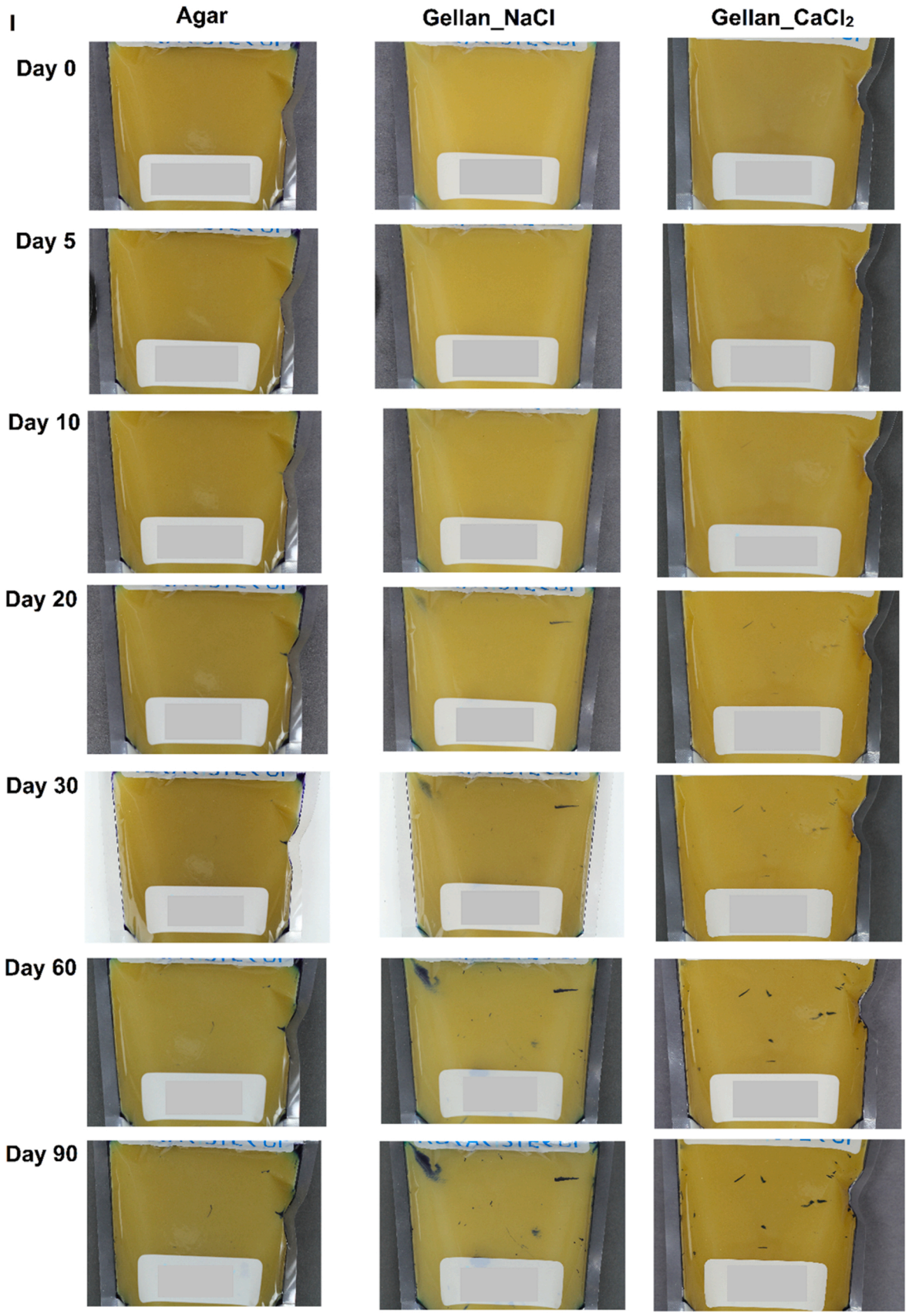

Fig. 3. Color change in gel-filled pouches; I–III, and A–C represent films A and B, respectively. I and A represent the unprocessed pouches stored at 23 ± 2 °C for 90 days; II and B represent R40-processed pouches stored at 23 °C for 90 days and III and C represent R40-processed pouches stored at 40 ± 0.2 °C for 90 days.

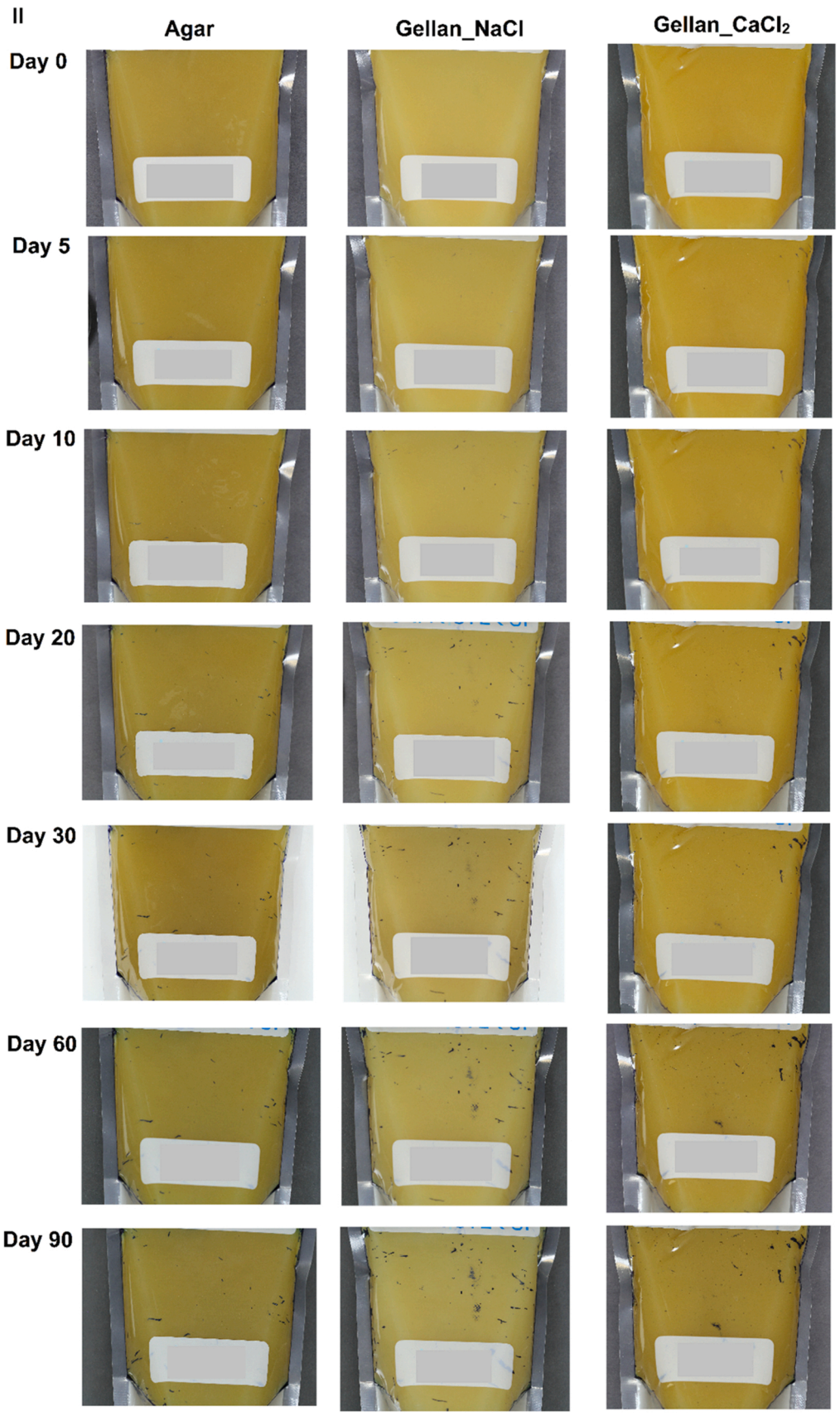

Fig. 3. (*continued*).

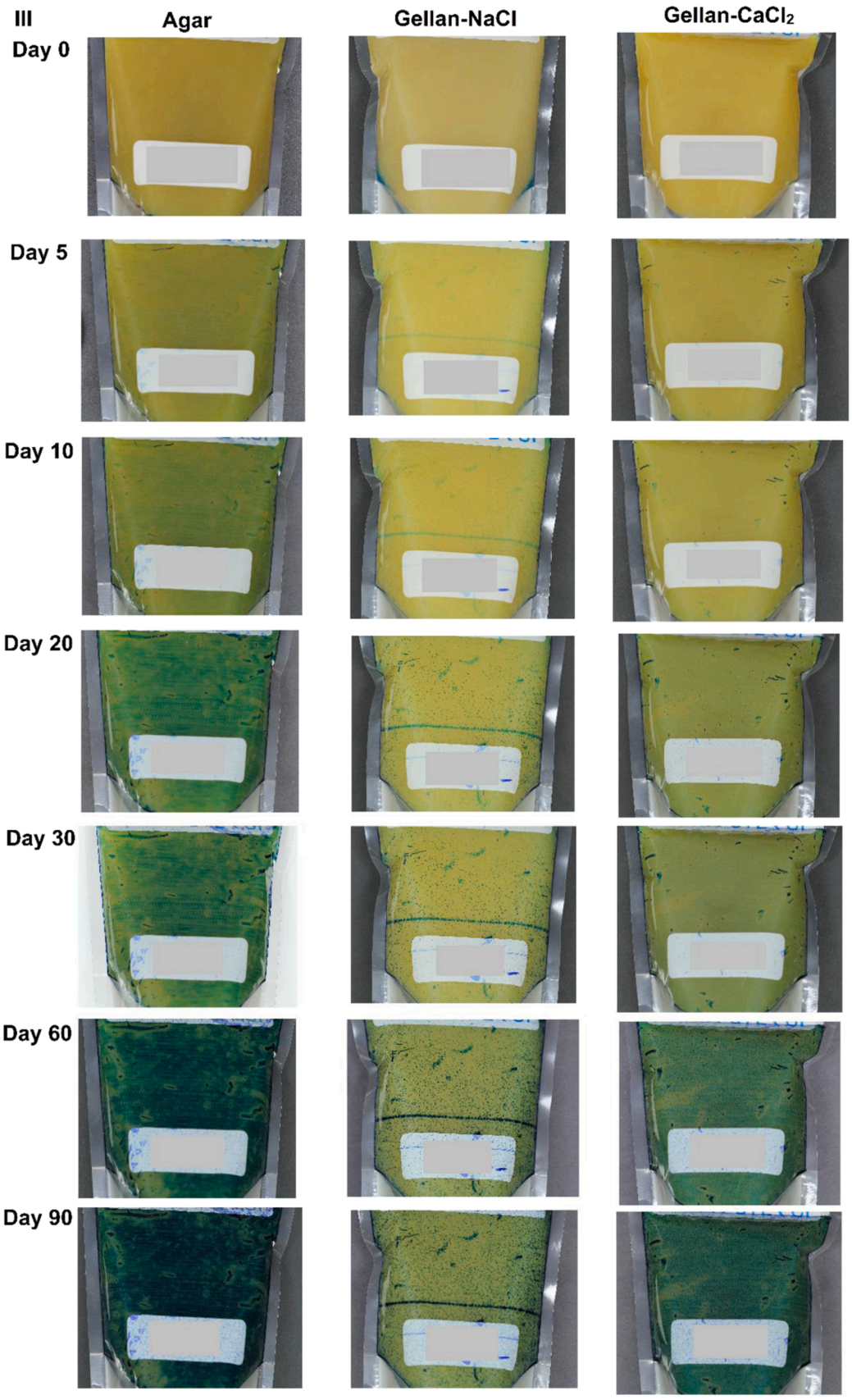

Fig. 3. (*continued*).

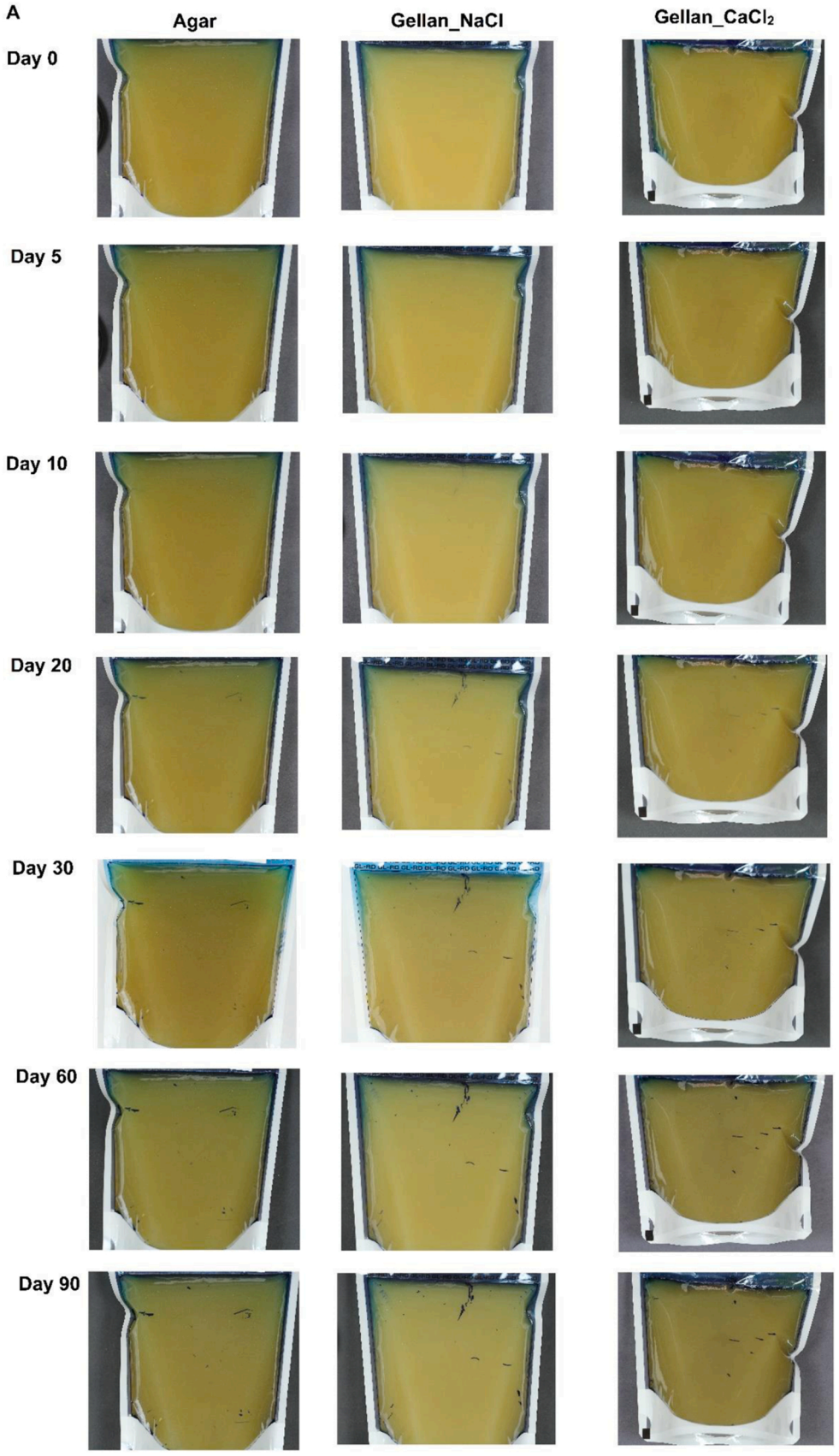

Fig. 3. (*continued*).

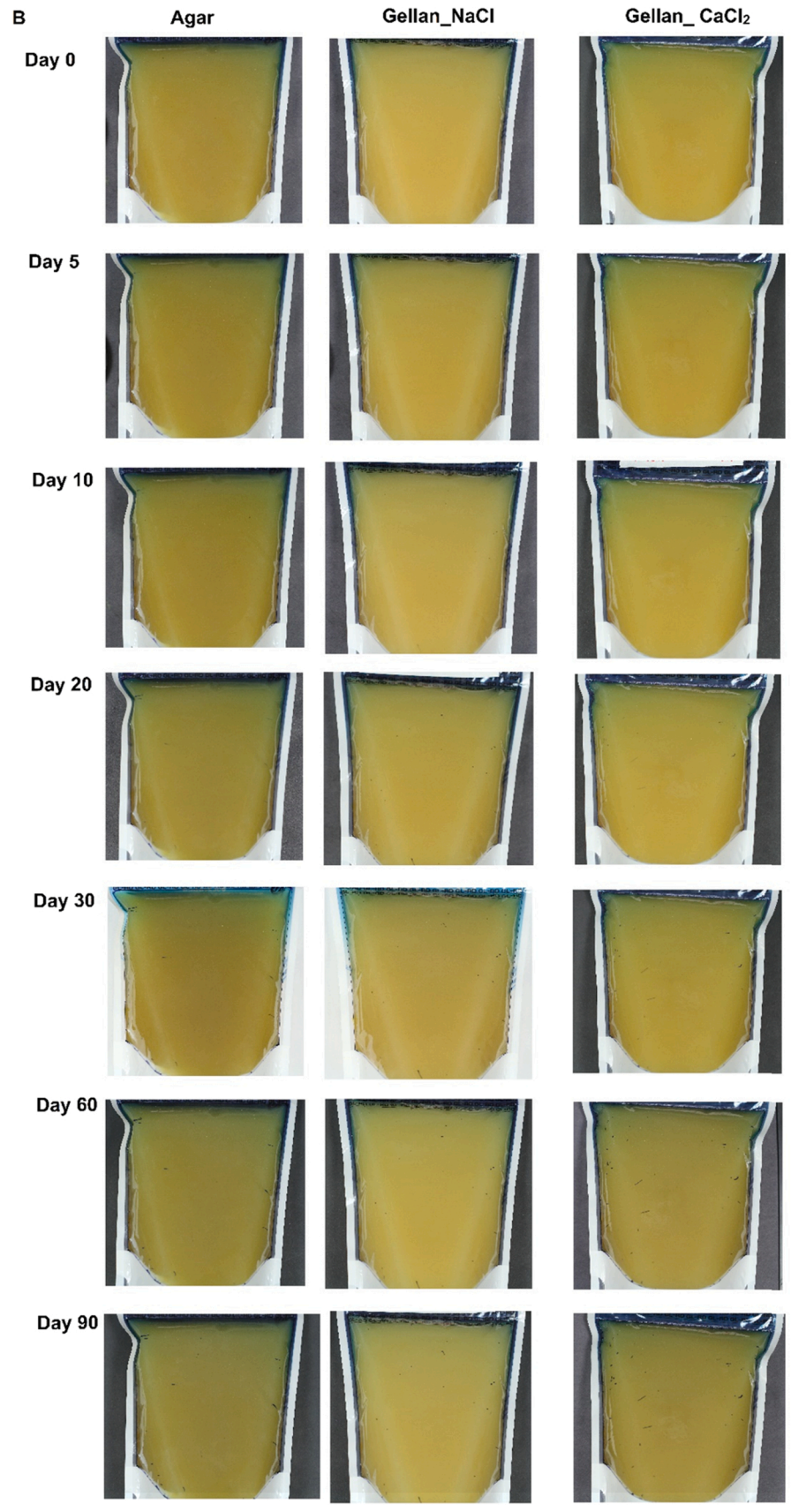

Fig. 3. (*continued*).

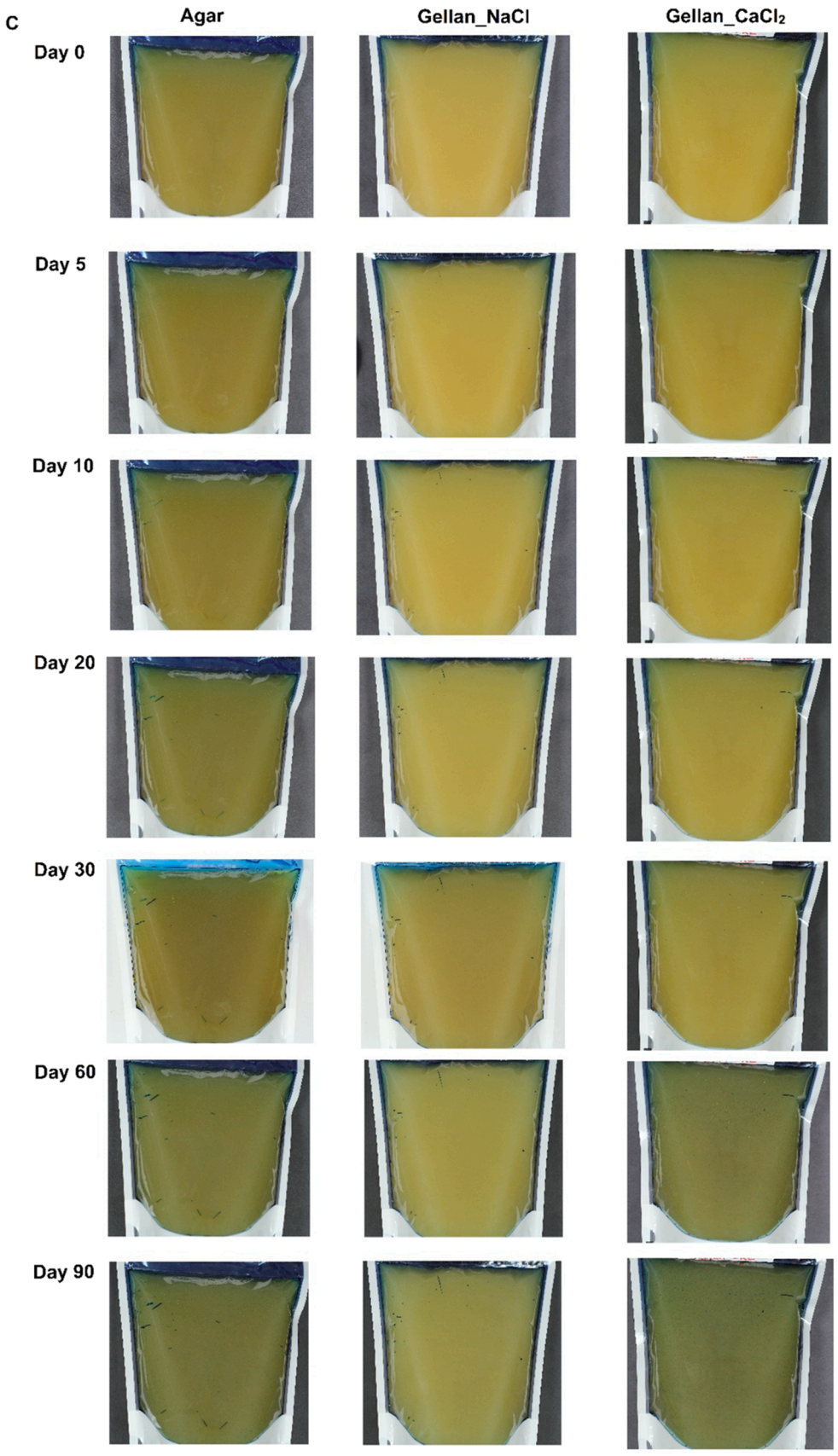

Fig. 3. (*continued*).

This increased the amount of oxygen reacting with the active elements in the packaged gels in film A pouches, causing an increased blueness. At the same time, the volumes of oxygen permeating through the SiO_x layer of film B were lesser than film A. Hence, the gels in film B showed a reduced blue coloration under similar storage conditions (Fig. 3). The pouches containing agar and Gellan_$CaCl_2$ started to turn blue by Day-10 at 40 ± 0.2 ℃ (Fig. 3). Agar gels turned blue even before most of the cracks and pinholes were identified. Gellan_$CaCl_2$ showed a similar trend by Day-60, while Gellan_NaCl was the best and held its color till the end at the defective locations. This is vital for detecting smaller defects as they take longer to be identified and create maximum barrier deterioration compared to a few larger cracks (Leterrier, 2003).

The gelation temperature of the gels can impact the detection process. Prior research has shown that the MB can be adsorbed by the deformations in inner PP layer of the multilayer films (Parhi et al., 2019). When the oxygen ingress happens through the pinholes and cracks in the coating, the MB present in the entrapped gels changes color. Gels such as Gellan gum have a higher gelation temperature (approx. 60 ℃) (Tang et al., 1994, 1997). This allows the gels present in the PP layer to remain immobilized at 40 ± 0.2 ℃, reducing blue coloration and thus facilitating an accelerated detection. However, in case of agar gels, detection at 40 ± 0.2 ℃ can be challenging considering its lower gelation temperature (35–37 ℃), which can cause the gels entrapped in the PP layers to leach out (Parhi et al., 2019). As a result, in this study, packaged gels with gellan gums had a reduced color intensity than agar.

4. Conclusions

This study illustrated that newly developed gels were effective at detecting the defects in MO-coated multilayer films under accelerated test conditions. Gellan_NaCl showed higher oxygen sensitivity than Gellan_$CaCl_2$ and agar. As a result, it worked well with films having both high and low OTRs. Gellan- NaCl changed color efficiently at the locations with the defects and did not affect the process of detection with any false positives. The gel had lower color diffusion and WR compared to agar and Gellan_$CaCl_2$. Thermal processing significantly increased the OTRs of the packaging films and this was reflected in the color change in the gels. Overall, oxygen sensitive Gellan_NaCl gel can accelerate the detection process of the defects in the MO-coated multilayer food packaging films used for shelf stable products needing longer storage.

Funding

This work was supported by the USDA National Institute of Food and Agriculture Research grants 2016-67017-24597, 2016-68003-24840 and Hatch project #1016366.

CRediT authorship contribution statement

Ashutos Parhi: Conceptualization, Data curation, Methodology, Formal analysis, Investigation, Writing - original draft, Writing - review & editing. **Chongyuan Zhang:** Methodology, Data curation, Writing - original draft. **Chandrashekhar R. Sonar:** Methodology, Conceptualization. **Sindhuja Sankaran:** Methodology, Writing - review & editing. **Barbara Rasco:** Methodology, Conceptualization, Writing - review & editing. **Juming Tang:** Methodology, Conceptualization, Writing - review & editing. **Shyam S. Sablani:** Funding acquisition, Conceptualization, Writing - original draft, Writing - review & editing.

Declaration of Competing Interest

The authors declare that they have no known competing financial interests or personal relationships that could have appeared to influence the work reported in this paper.

Data Availability

Data will be made available on request.

Acknowledgements

The authors thank the polymer companies for supplying the film pouches.

References

Anderson, L., Wittkopp, S. M., Painter, C. J., Liegel, J. J., Schreiner, R., Bell, J. A., & Shakhashiri, B. Z. (2012). What is happening when the blue bottle bleaches: An investigation of the methylene blue-catalyzed air oxidation of glucose. *Journal of Chemical Education, 89*(11), 1425–1431. https://doi.org/10.1021/ed200511d

Banerjee, S., & Bhattacharya, S. (2011). Compressive textural attributes, opacity and syneresis of gels prepared from gellan, agar and their mixtures. *Journal of Food Engineering, 102*(3), 287–292. https://doi.org/10.1016/j.jfoodeng.2010.08.025

Bhunia, K., Sablani, S. S., Tang, J., & Rasco, B. (2016). Non-invasive measurement of oxygen diffusion in model foods. *Food Research International, 89*, 161–168. https://doi.org/10.1016/j.foodres.2016.07.015

Bhunia, K., Zhang, H., Liu, F., Rasco, B., Tang, J., & Sablani, S. S. (2016). Morphological changes in multilayer polymeric films induced after microwave-assisted pasteurization. *Innovative Food Science & Emerging Technologies, 38*, 124–130. https://doi.org/10.1016/j.ifset.2016.09.024

Campbell, J. A. (1963). Kinetics—early and often. *Journal of Chemical Education, 40*(11), 578. https://doi.org/10.1021/ed040p578

Cassanelli, M., Prosapio, V., Norton, I., & Mills, T. (2019). Role of the drying technique on the low-acyl gellan gum gel structure: molecular and macroscopic investigations. *Food and Bioprocess Technology, 12*(2), 313–324. https://doi.org/10.1007/s11947-018-2210-6

Henry, B. M., Erlat, A. G., McGuigan, A., Grovenor, C. R. M., Briggs, G. A. D., Tsukahara, Y., Miyamoto, T., Noguchi, N., & Niijima, T. (2001). Characterization of transparent aluminium oxide and indium tin oxide layers on polymer substrates. *Thin Solid Films, 382*(1–2), 194–201. https://doi.org/10.1016/S0040-6090(00)01769-7

Leterrier, Y. (2003). Durability of nanosized oxygen-barrier coatings on polymers. *Progress in Materials Science, 48*(1), 1–55. https://doi.org/10.1016/S0079-6425(02)00002-6

Leterrier, Y., Månson, J.-A. E., & Wyser, Y. (2001). Internal stresses and adhesion of thin silicon oxide coatings on poly(ethylene terephthalate. *Journal of Adhesion Science and Technology, 15*(7), 841–865. https://doi.org/10.1163/15685610152540885

Mao, R., Tang, J., & Swanson, B. G. (1999). Efect of pH buffers on mechanical properties of gellan gels. *Journal of Texture Studies, 30*(2), 151–166. https://doi.org/10.1111/j.1745-4603.1999.tb00208.x

Mao, R., Tang, J., & Swanson, B. G. (2001). Water holding capacity and microstructure of gellan gels. *Carbohydrate Polymers, 46*(4), 365–371. https://doi.org/10.1016/S0144-8617(00)00337-4

Nishinari, K., & Fang, Y. (2016). Sucrose release from polysaccharide gels. *Food & Function, 7*(5), 2130–2146. https://doi.org/10.1039/C5FO01400J

Parhi, A., Bhunia, K., Rasco, B., Tang, J., & Sablani, S. S. (2019). Development of an oxygen sensitive model gel system to detect defects in metal oxide coated multilayer polymeric films. *Journal of Food Science, 1750–3841*, 14755. https://doi.org/10.1111/1750-3841.14755

Parhi, A., Tang, J., & Sablani, S. S. (2020). Functionality of ultra-high barrier metal oxide-coated polymer films for in-package, thermally sterilized food products. *Food Packaging and Shelf Life, 25*, Article 100514. https://doi.org/10.1016/j.fpsl.2020.100514

Picone, C. S. F., & Cunha, R. L. (2011). Influence of pH on formation and properties of gellan gels. *Carbohydrate Polymers, 84*(1), 662–668. https://doi.org/10.1016/j.carbpol.2010.12.045

Roberts, A. P., Henry, B. M., Sutton, A. P., Grovenor, C. R. M., Briggs, G. A. D., Miyamoto, T., Kano, M., Tsukahara, Y., & Yanaka, M. (2002). Gas permeation in silicon-oxide/polymer (SiOx/PET) barrier films: Role of the oxide lattice, nano-defects and macro-defects. *Journal of Membrane Science, 208*(1–2), 75–88. https://doi.org/10.1016/S0376-7388(02)00178-3

Tang, J., Lelievre, J., Tung, M. A., & Zeng, Y. (1994). Polymer and ion concentration effects on gellan gel strength and strain. *Journal of Food Science, 59*(1), 216–220. https://doi.org/10.1111/j.1365-2621.1994.tb06934.x

Tang, J., Tung, M. A., & Zeng, Y. (1995). Mechanical properties of gellan gels in relation to divalent cations. *Journal of Food Science, 60*(4), 748–752. https://doi.org/10.1111/j.1365-2621.1995.tb06220.x

Tang, J., Tung, M. A., & Zeng, Y. (1997). Gelling properties of gellan solutions containing monovalent and divalent cations. *Journal of Food Science, 62*(4), 688–712. https://doi.org/10.1111/j.1365-2621.1997.tb15436.x